Diagnostic and intraoperative targeted molecular imaging for pancreatic cancer

Tummers, W.S.F.J.

Chapter | 11

Detection of Visually Occult Metastatic Lymph Nodes Using Molecularly Targeted Fluorescent Imaging During Surgical Resection of Pancreatic Cancer

Willemieke S Tummers, MD [1 2], Sarah E Miller, B.S. [3], Nutte T Teraphongphom, Ph.D. [3], Nynke S. van den Berg, Ph.D. [3], Alifia Hasan, M.B.A. [3], Teri A Longacre, MD [4], George A Fisher, MD [5], Bert A Bonsing, MD, Ph.D. [2], Alexander L Vahrmeijer, MD, Ph.D. [2], Sanjiv S Gambhir, MD, Ph.D. [6], Rutger-Jan Swijnenburg MD, Ph.D. [2], Eben L Rosenthal, M.D., F.A.C.S. [3], George A Poultsides, MD [7].

[1] Department of Radiology, Molecular Imaging Program at Stanford (MIPS), Stanford University, Stanford, CA, 94305, USA. [2] Department of Surgery, Leiden University Medical Center, Albinusdreef 2, 2300 RC, Leiden, the Netherlands. [3] Department of Otolaryngology, Stanford University, Stanford, CA. [4] Department of Pathology, Stanford University, Stanford, CA. [5] Department of Medical Oncology, Stanford University, Stanford, CA. [6] Departments of Radiology, Bioengineering, and Materials Science & Engineering, Molecular Imaging Program at Stanford. Canary Center at Stanford for Early Cancer Detection. Stanford University, Stanford, CA, 94305, USA. [7] Department of Surgery, Stanford University, Stanford, CA.

ABSTRACT

Objective: To examine the efficacy of molecularly targeted intraoperative fluorescent imaging in the detection of metastatic lymph nodes (LNs) during resection of pancreatic ductal adenocarcinoma (PDAC).

Summary Background Data: Although most patients with PDAC experience distant failure after resection, a significant portion still present with local recurrence. Intraoperative fluorescent imaging can potentially facilitate the visualization of involved peritumoral LNs and guide the locoregional extent of nodal dissection enabling staging and complete tumor clearance.

Methods: A dose-escalation prospective study was performed to assess the feasibility of tumor detection within peripancreatic LNs using cetuximab-IRDye800 in PDAC patients undergoing surgical resection. Patients received either 50 mg or 100 mg of cetuximab-IRDye800 2-5 days preoperatively. Fluorescent imaging of dissected LNs was analysed *ex vivo* macroscopically and microscopically and fluorescence was correlated with histopathology.

Results: A total of 144 LNs (72 in the low-dose and 72 in the high-dose cohort) were evaluated in 7 patients. Detection of metastatic LNs by fluorescence was better in the low-dose (50 mg) cohort, where sensitivity and specificity was 100% and 78% macroscopically, and 91% and 66% microscopically. More importantly, this method was able to detect occult foci of tumor (measuring < 5 mm) with a sensitivity of 88% (15/17 LNs).

Conclusion: This study provides proof of concept that intraoperative fluorescent imaging with cetuximab-IRDye800 can facilitate the detection of peripancreatic lymph nodes often containing subclinical foci of disease. This method holds promise in enhancing nodal tumor detection during surgery for PDAC, enabling more precise and targeted lymphadenectomy.

INTRODUCTION

Pancreatic Ductal Adenocarcinoma (PDAC) represents a significant challenge in surgery and oncology. Autopsy studies have identified that although 70% of patients with pancreatic cancer die of widespread metastases, a significant portion (30%) die of locally destructive disease.[1] Therefore, although PDAC is largely considered a systemic disease at presentation, efforts to improve local therapies are very important. For patients with locally contained disease, surgery is the mainstay of management and the only chance for cure. Thus, maximizing the completeness of surgical resection in this setting is critical. However, even following what is felt to be a curative-intent resection, up to a third of patients with PDAC die from disease within a year from surgery.[2] This early failure is related mostly to unrecognized distant disease at the time of surgery, but also to residual disease left in situ at the resection bed. This occult residual disease is often below the threshold of detection by current intraoperative or radiologic imaging modalities. We have previously shown that tumor-specific imaging using a fluorescent dye targeting epidermal growth factor receptors (EGFR) on the tumor, especially in the form of intraoperative fluorescence imaging, has high sensitivity and specificity even for low-volume PDAC.[3-5]

The use of intraoperative fluorescence imaging can potentially improve the operative management of PDAC patients, since the extent of locoregional dissection can be expanded, to lymph node clearance. Sites of peritumoral lymphatics that can potentially be left behind after pancreatectomy, but are still considered locoregional sites of disease, are shown in Figure 1. The effect of additional lymph node resection remains subject to debate, as four previously published randomized trials have shown that extended lymphadenectomy for "all comers" undergoing PDAC resection does not provide therapeutic benefit.[6-10] However, these trials pertain to all presenting patients with resectable PDAC and it remains unclear whether precision surgery, (utilizing fluorescence guidance as part of the lymph node dissection to target occult nodes in the resection bed) could improve long-term surgical outcomes for this disease. To this end, we hypothesize that with intraoperative identification of occult metastatic lymph nodes using tumor-specific imaging, either a targeted lymph node dissection could be performed (should these nodes are considered regional), or

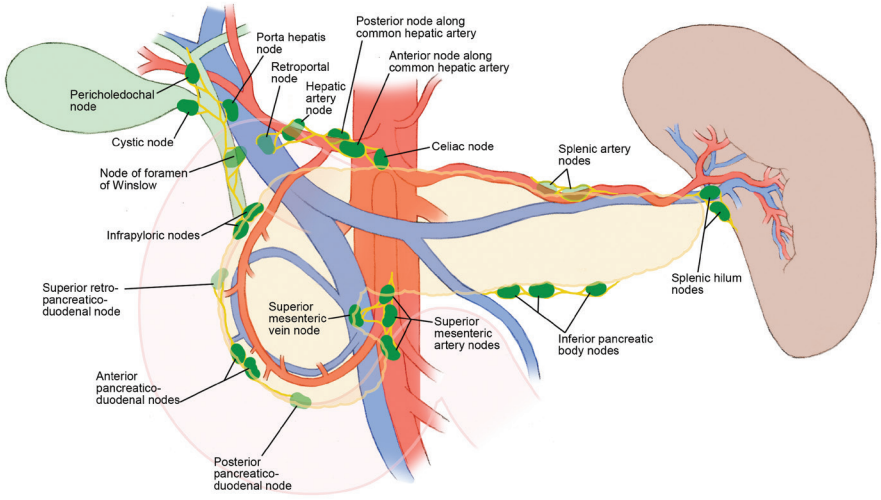

Figure 1. **Locoregional peripancreatic lymph nodes**. Involved lymph nodes in periaortic locations or high up in the hepatoduodenal ligament towards the liver would be considered distant metastatic disease during surgery for PDAC.

the resection could be aborted (if these nodes are considered M1 disease) if no oncologic benefit is anticipated from resection.

For tumor-specific molecular imaging, a biomarker is needed to be able to target tumor tissue. We have previously demonstrated in a cohort of 129 patients with different stages of PDAC that EGFR was abundantly expressed in up to 70% of cases.[11] To validate these results, we also tested the marker on tissues of patients with chronic pancreatitis and in lymph node metastases.[12] These experiments confirmed that EGFR is an appropriate pancreatic cancer-specific marker, also able to differentiate between benign and malignant pancreatic lesions, and detect tumor-positive lymph nodes. Interestingly, only low levels of EGFR expression are required for imaging,[13] which supports our hypothesis that small tumor burden in lymph nodes can be detectable by fluorescence.

We recently reported on the results of a prospective study utilizing EGFR-targeting cetuximab-IRDye800 for intraoperative fluorescent imaging of the pancreatic primary tumor during resection of PDAC.[5] In the current analysis, we

focus specifically on the diagnostic accuracy of this method for tumor-specific lymph node detection.

MATERIALS AND METHODS

Study design

The study was performed as a single-arm, open-label, dose-escalation study, with the main objective of determining the safety and feasibility of tumor-specific multimodal molecular imaging for detection of PDAC, as described previously.[5] Briefly, patients with suspected or biopsy-proven PDAC scheduled to undergo surgical resection at Stanford University Hospital were identified. A dose-escalation model using two doses (50 mg and 100 mg) of cetuximab-IRDye800 was chosen to identify the dose providing optimal tumor detection. The doses were determined based on previous findings by our group showing that a dose of 62.5 mg/m^2 provided the optimal tumor-to-background ratio (TBR) for head and neck cancer.[4] After informed consent, patients received a systemic infusion of the study drug 2-5 days before surgery. A pretreatment loading dose of 100 mg unlabeled cetuximab was administered before cetuximab-IRDye800 to differentiate between an infusion reaction to the parent compound (cetuximab) and a cetuximab-IRDye800 reaction, and also to preload the EGFR receptors in the liver.[14] After a 3-hour observation period, the patients were discharged and returned for surgery 2-5 days later.

Investigational agent: cetuximab-IRDye800

The study drug (cetuximab-IRDye800) was produced under clinical Good Manufacturing Practice (cGMP) conditions at the University of Alabama (UAB) Vector Production Facility as previously described,[15] before shipment to Stanford University Hospital Pharmacy. During transit the temperature was monitored and kept stable. Briefly, cetuximab (ImClone LLC, Eli Lilly and Company) was concentrated and pH adjusted by buffer exchange to a 10mg/mL solution in 50 mmol/L potassium phosphate, pH 8.5. IRDye800CW NHS ester (LI–COR Biosciences) was conjugated to cetuximab for 2 hours at 20°C in the dark, at a molar ratio of 2.3:1.

Optical imaging

Intraoperative near-infrared (NIR) imaging

Intraoperative imaging of the operative field in real time was performed using the wide-field SurgVision Explorer (SurgVision BV, 't Harde, The Netherlands) at 3 time points: during preliminary inspection of the abdomen, after initial dissection but before tumor resection, and after tumor resection. The surgical specimen was processed by the pathologist according to standard clinical practice for inking, sectioning and margin evaluation. During this preliminary study, the findings of intraoperative imaging did not inform intraoperative management, which otherwise followed standard contemporary practice for patients with PDAC.

Closed-field near-infrared (NIR) ex vivo imaging

Closed-field NIR *ex vivo* imaging was performed using The Pearl Impulse imaging platform (LI–COR Biosciences, Lincoln, NE) as previously described [5]. Briefly, the system was used to image fresh tissue obtained in the operating room prior to paraffin embedding. In addition, the system was used to measure mean fluorescence intensity (MFI) of the tumor and surrounding background tissue. MFI was defined as total counts/region of interest (ROI) pixel area, using integrated instrument software (ImageStudio, LI–COR Biosciences). After measuring the signal intensity from macroscopic images, the following formula was used to measure Tumor to Background Ratio (TBR) = MFI of the tumor/ MFI of the surrounding tissue.

Pathologic assessment

All resected specimens were examined by a single dedicated gastrointestinal pathologist (TAL) with expertise in pancreatic disease. Formalin-fixed paraffin-embedded tumor tissues were sectioned at 4 μm thickness and fluorescence imaging was performed using the Odyssey NIR scanner (Li-COR Biosciences). The system was used to determine microscopic accuracy of fluorescence, correlated to standard hematoxylin-eosin (H&E) staining. NIR-fluorescence measurements were done following the same method as described above, using the integrated instrument software ImageStudio.

To confirm the presence of EGFR, additional sections underwent immunohistochemical (IHC) analysis for EGFR expression using anti-human EGFR

monoclonal antibodies (predilute, rabbit, clone 5B7, 790-4347, Ventana, Tucson, AZ). Automated immunohistochemical staining was performed with Ventana Benchmark XT (Ventana Medical Systems, Inc., Tucson, AZ, USA). Formalin fixed paraffin embedded (FFPE) tissue sections cut at 4 µm were deparaffinized and rehydrated. Antigen retrieval was performed by heat pretreatment at Standard Cell Conditioning 1 (Ventana Tris/ Borate/ EDTA-based buffer at pH 8.5) for 60 minutes. The slides were incubated with primary antibodies at 37°C for 32 minutes. After primary incubation, ultraView Universal DAB Detection system (Ventana) was used for single brown staining with 3,3'diaminobenzidine chromogen.

Ethics approval

The described study is performed in accordance with the tenets established by the Helsinki Declaration of 1975 (as amended in Tokyo, Venice, Hong Kong, Somerset West, Edinburgh, Washington, and Seoul), ICH-GCP guidelines, and the laws and regulations of the United States. The Stanford University Institutional Review Board and the FDA approved the study protocol. All patients provided written informed consent. The study was registered in the Clinical Trials Database of the U.S. National Institutes of Health, under number NCT02736578.

Statistical analysis

SPSS statistical software package (version 23.0, IBM Corp.) was used for statistical analyses, and GraphPad Prism 7 (version 7.02, GraphPad Sorftware, Inc.). Differences in fluorescent signal between tumor-positive and tumor-negative lymph nodes were tested separately and between different dose groups, with One-way ANOVA with posthoc Bonferroni correction. TBR is reported as the mean, SEM, and range. Graphical display was performed using box plot graphs, and Receiver Operating Characteristic (ROC) curves.

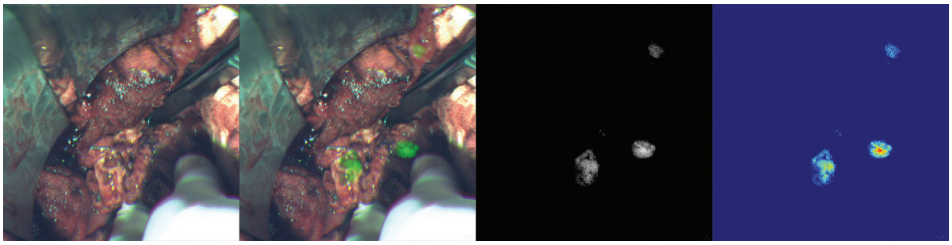

Figure 2. Intraoperative lymph node detection. Tumor-positive lymph nodes in the hepatoduodenal ligament during pancreaticoduodenectomy. Bright field image of wound bed (2A), overlay (2B), grayscale (2C), and heat-map (2D) fluorescence imaging provided clear contrast between tumor and surrounding tissue. Imaging was performed with wide-field SurgVision Explorer (SurgVision BV, 't Harde, The Netherlands).

RESULTS

Metastatic lymph node detection using cetuximab-IRDye800

A total of 144 lymph nodes were evaluated in the 7 patients; in the low-dose cohort (50 mg), there were 72 nodes evaluated of which 64 were tumor-negative and 8 were tumor-positive. In the high-dose (100 mg) cohort, a total of 72 nodes was evaluated of which 56 were tumor-negative and 16 were tumor-positive. Examples of tumor-positive lymph nodes detected in real-time by fluorescence during surgery are shown in Figure 2.

For the entire cohort, tumor-positive lymph nodes could be detected *ex vivo* demonstrating significantly higher MFI (0.06±0.01) compared to tumor-negative lymph nodes (0.02±0.002) ($p<0.001$). This difference was more pronounced in the low-dose cohort, where MFI for tumor-positive lymph nodes was 0.071, compared to 0.018 for tumor-negative lymph nodes ($p<0.001$) (Figure 3A). In contrast, in the high-dose cohort, the difference in MFI between tumor-positive lymph nodes and tumor-negative lymph nodes was not significant (0.046 vs.0.035, $p=0.148$) (Figure 3B). The sensitivity to detect tumor-positive lymph nodes in the low-dose cohort was 100% (C.I. 73.5 – 100) and specificity 78% (C.I. 64.0 – 88.5), with a likelihood ratio of 4.55. In the high-dose cohort, the sensitivity was 88.2% (C.I. 63.6 – 98.5) and specificity decreased to 32.1% (C.I. 15.9 – 52.4), with a likelihood ratio of 1.30 (Figure 3C).

Fluorescence intensity of formalin-fixed paraffin-embedded tissue sections were evaluated to validate tumor targeting of the fluorescent agent. A significant

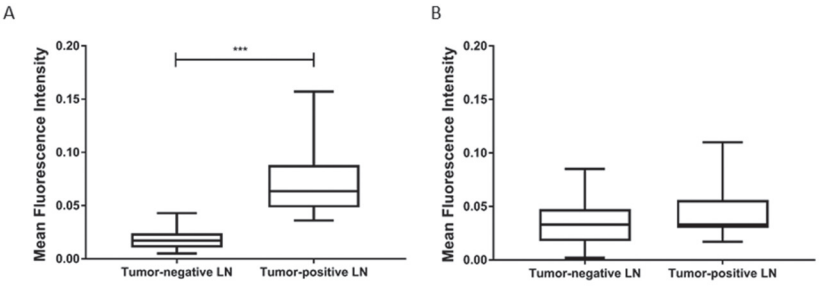

C

	Low dose	High dose
Sensitivity (95% C.I.)	100% (73.5 – 100)	88.2% (63.6 – 98.5)
Specificity (95% C.I.)	78% (64.0 – 88.5)	32.1% (15.9 – 52.4)
AUC	0.99 (0.98 – 1.00)	0.58 (0.41 – 0.76)
Likelihood ratio	4.55	1.30

Figure 3. Detection of tumor-positive lymph nodes using fluorescence imaging of fresh tissue ex vivo. Analyzing the low-dose cohort, MFI for tumor-positive lymph nodes was 0.071, compared to 0.018 for tumor-negative lymph nodes (p<0.001) (Figure 3A). In the high-dose cohort, the MFI for tumor-positive lymph nodes was 0.046, compared to 0.035 for tumor-negative lymph nodes (p=0.148) (Figure 3B). Images were obtained with The Pearl Impulse imaging platform (LI–COR Biosciences, Lincoln, NE), and MFI was determined with integrated software (ImageStudio, LI–COR Biosciences). Test characteristics of fluorescence for the detection of tumor-positive lymph nodes are shown in Figure 3C.

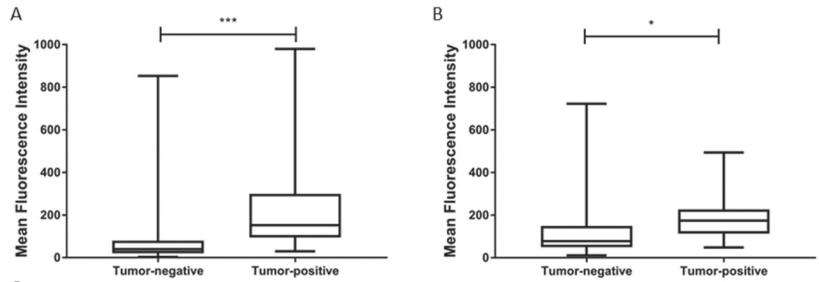

C

	Low dose	High dose
Sensitivity (95% C.I.)	91.4% (76.4 – 96.4)	93.1% (77.2 – 99.2)
Specificity (95% C.I.)	66.3% (61.6 – 70.8)	34.8% (26.2 – 44.1)
AUC	0.84 (0.79 – 0.89)	0.73 (0.64 – 0.82)
Likelihood ratio	2.64	1.43

Figure 4. Detection of tumor-positive lymph nodes using fluorescent imaging of formalin-fixed paraffin-embedded tissue sections. In the low-dose cohort, a significant difference was seen between the MFI of tumor-positive lymph nodes (250.4±33.9) and tumor-negative lymph nodes (76.4±5.1) (p<0.001) (Figure 4A). The same was true for the high-dose cohort, with the fluorescence in tumor-positive lymph nodes being 182.5±19.0 and in tumor-negative lymph nodes 126.9±11.9 (p=0.03) (Figure 4B). Images were obtained with the Odyssey NIR scanner (Li-COR Biosciences), and MFI was determined with integrated software (ImageStudio, LI–COR Biosciences). Test characteristics for the detection of tumor using fluorescence at the microscopic level per dose group are shown in Figure 4C.

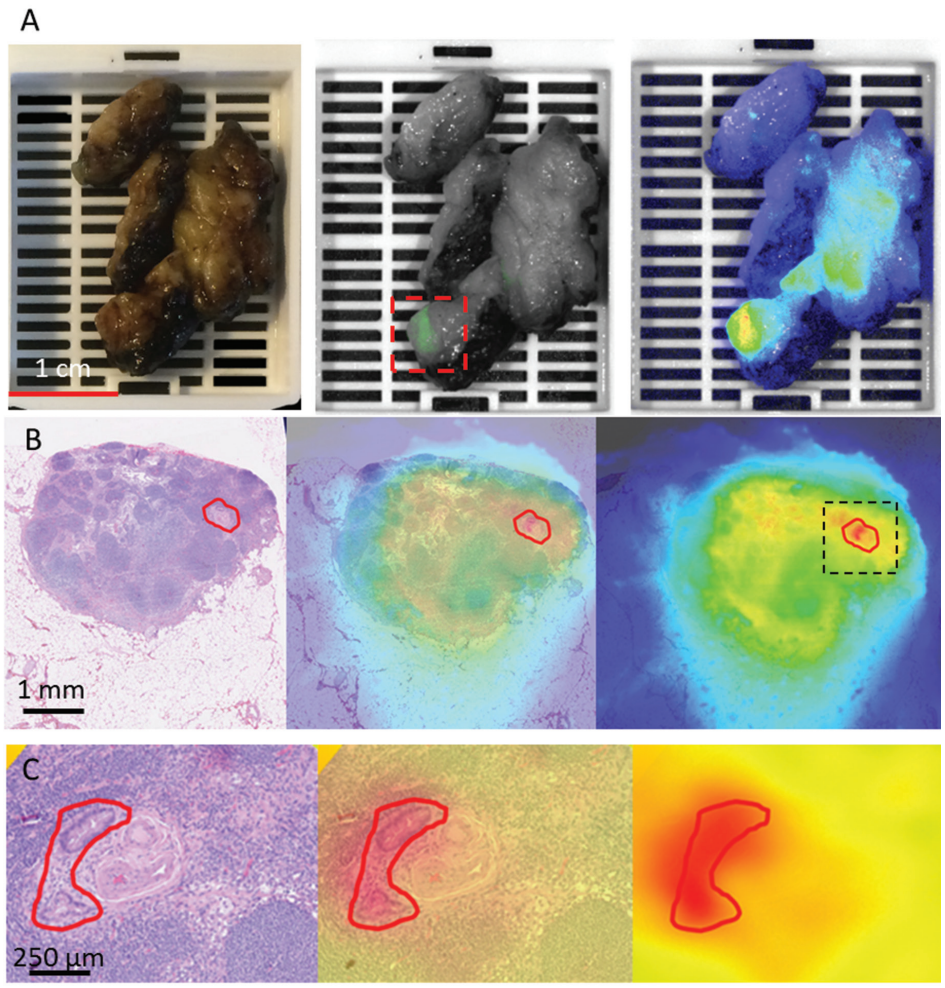

Figure 5. Detection of occult tumor deposits within lymph nodes. Figure 5A shows resected peripancreatic fat with an embedded lymph node ex vivo in bright light, overlay fluorescence mode, and heat-map fluorescence mode (respectively from left to right). In figure 5B the fluorescence part (red dotted box) is visualized at the microscopic level with the tumor section outlined. An overlay is created between the H&E and the fluorescence image in three steps showing high fluorescence only at the location of the occult tumor (black dotted box). In figure 5C, the two tumor foci are visualized in more detail with the same method of overlaying the H&E and fluorescence image, demonstrating the ability of fluorescence to detect tumor deposits of only 0.5 x 0.25 mm in size.

difference in MFI was seen in the low-dose cohort between tumor-positive lymph nodes (250.4±33.9) and tumor-negative lymph nodes (76.4±5.1) ($p<0.001$) (Figure 4A). The same was true for the high-dose cohort, but a smaller difference in MFI between tumor-positive and tumor-negative lymph nodes (182.5±19.0 and

126.9±11.9, respectively) was noted (p=0.03) (Figure 4B). The test characteristics for the microscopic detection of tumor using targeted fluorescence imaging for the low-dose cohort included sensitivity of 91.4% (C.I. 76.4 – 96.4) and specificity of 66.3% (C.I. 61.6 – 70.8). In the high-dose cohort, the specificity was relatively low due to high frequencies of false-positive detection in the lymph nodes (34.8%, C.I. 26.2 – 44.1), though sensitivity was higher (93.1%, 77.2 – 99.2) (Figure 4C).

Imaging of occult tumor in lymph nodes

For intraoperative fluorescence to augment current intraoperative techniques used by the surgeon (palpation, inspection), it should allow for the detection of subclinical/occult tumors. Therefore, it is important that even lymph nodes that contain "microscopic" amounts of tumor can be detected by fluorescence (Figure 5A). When analyzing the fluorescence data at the microscopic level, even sub-millimeter tumor lesions of 0.25 by 0.5 mm (e.g. 2 tumor glands in close proximity) were detected using fluorescence (Figure 5B and 5C). Of the 17 lymph nodes with "occult" tumor (defined as tumor foci < 5 mm in size), 15 were detected by fluorescence, and 2 were not, resulting in a sensitivity of 88.2%. The amount of tumor in the two non-fluorescent lymph nodes was comparable to the fluorescent lymph nodes (0.83 mm vs 1.98 mm, p = 0.425).

Non-specific drainage of fluorescent agent

In the high dose cohort, a significant amount of false-positive lymph nodes were seen. Additional sectioning and pathologic analysis of these false-positive nodes did not reveal occult tumor not identified at initial pathological review. We, therefore, hypothesized that this was due to the tumor-bound cetuximab-IRDye800 leaking non-specifically out of the tumor, into the regional lymphatic nodal basin. To examine this hypothesis, we looked into the localization of fluorescence within these false-positive lymph nodes and the relationship with D2-40 immunostaining (a marker of lymphatic endothelium). We identified that areas of high (false-positive) fluorescence corresponded to enlarged lymphatics, as highlighted by D2-40 staining (Figure 6).

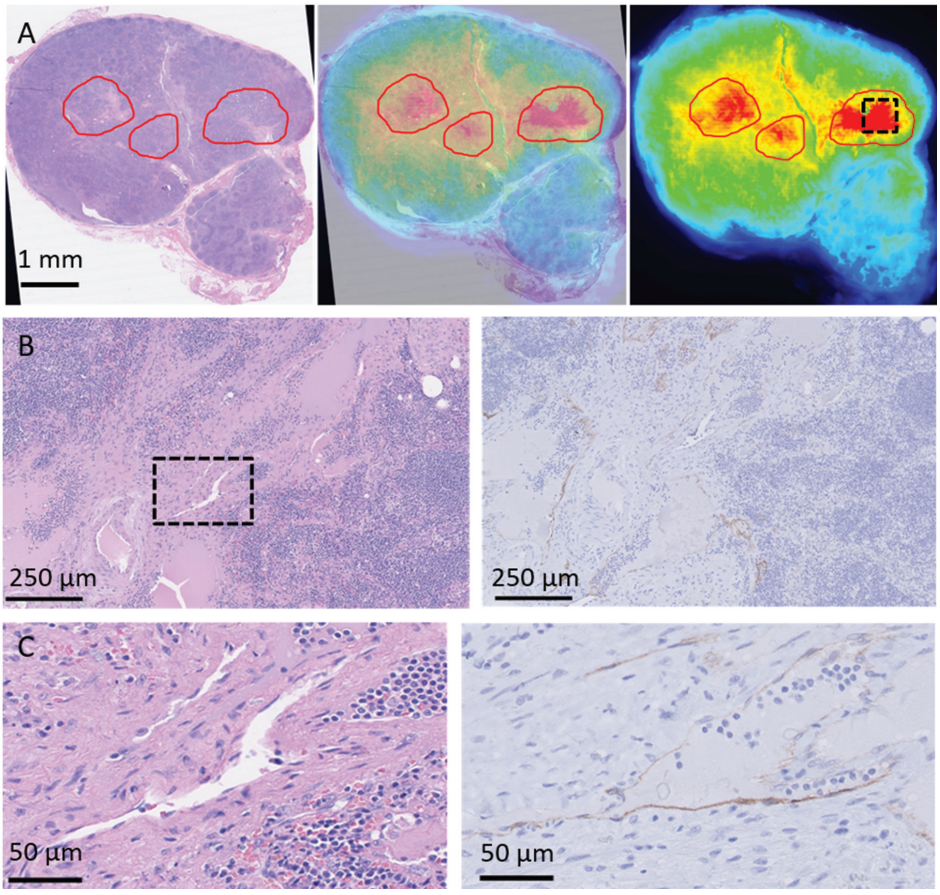

Figure 6. Non-specific drainage pattern in false-positive lymph nodes. Fluorescence and H&E overlays are shown with high fluorescence at position of lymphatic vessels (Figure 6A) in a patient who received the high-dose (100 mg) of cetuximab-IRdye800. In Figure 6B, a magnification of an area with high fluorescence (black dotted box) is shown, together with a D2-40 immunostain, which is a marker of lymphatic epithelium. In figure 6C this area is magnified further to shown co-localization of D2-40 staining (Figure 6C).

DISCUSSION

In this prospective dose escalation study of patients undergoing pancreatectomy for PDAC, we showed that in the low-dose cohort (50 mg of cetuximab-IRDye800) tumor-targeted fluorescent imaging identified tumor-positive lymph nodes *ex vivo* with a sensitivity of 100% and specificity of 78%. At the microscopic level, the sensitivity of the method was 91% and specificity was 66%. If the

high-sensitivity of this method can be replicated *in vivo* with improved surgical imaging equipment, this information can be used to improve intraoperative management and decision making. Specifically, if the fluorescently detected (but otherwise occult) node is located at distant site (and is conformed to be involved on frozen section), the resection can be aborted. Alternatively, if the detected node is considered locoregional, the resection can be extended to include this nodal basin and achieve a more complete resection.

Four prospective randomized trials, two from the US,[6-8] one from Europe[10] and one from Asia[9] have previously tried to answer the question of whether an extended lymph node dissection - including periaortic, renal hilum, upper hepatoduodenal, celiac, and superior mesenteric artery (N2) nodes – for all patients undergoing surgery for PDAC is associated with oncologic benefit. In aggregate, these studies included 424 patients and showed that the number of resected lymph nodes was significantly higher in the pancreaticoduodenectomy with extended lymphadenectomy group compared with the standard lymph node dissection group. Morbidity and mortality rates were comparable. In none of these trials, however, was a benefit in long-term survival demonstrated with extended lymphadenectomy. In accordance with these studies, we do not advocate routine performance of extended lymph node dissection in patients undergoing resection of PDAC. However, we view intraoperative molecularly targeted fluorescent imaging as a tool to identify the subset of patients with tumor-positive nodes remaining in the resection bed. The surgeon can proceed with their resection if they are felt to be locoregional sites of disease. In two of the aforementioned trials,[6-8] metastasis was noted in 15% and 29% of these second-order (N2 nodes) in the extended lymphadenectomy group. We feel that intraoperative fluorescent imaging may be a promising tool that can identify this exact subset of patients where disease would have otherwise been left in situ in the resection bed after a standard resection/lymphadenectomy, and where additional nodal dissection may ensure a more complete resection. Along the same lines, this “extended” lymphadenectomy does not have to be comprehensive to include all aforementioned N2 lymph node stations, but selective and targeted to include only the fluorescent nodes, thereby minimizing the potential complications and adverse events associated with more aggressive lymph node dissections. We envision this tool as a step closer to precision medicine in pancreatic cancer surgery. Whether this approach of

"precision lymphadenectomy" will be associated with improved long-term survival remains to be determined, however, it is interesting to note that the study of Pedrazzoli et al. showed improved survival for patients undergoing extended lymphadenectomy in an a *posteriori* subset analysis of patients with positive lymph nodes.[10]

Our method of molecularly-targeted fluorescent intraoperative imaging had relatively high sensitivity, but lower specificity for PDAC. Since fluorescent lymph nodes (in M1 sites) would routinely be checked with frozen section analysis during surgery to confirm the presence of cancer before further management decisions are made intraoperatively, we feel that the high number of false-positive lymph nodes is preferred to prevent the possibility of missing occult disease. In addition, one can hypothesize that these nodes may serve as sentinel lymph nodes (the first echelon of lymph nodes to which the tumor drains) in pancreatic cancer surgery with several clinical applications down the line. On the other hand, our method's high sensitivity is extremely important for any intraoperative guidance tool, as the lack of fluorescence in the resection bed (or other distant sites) would be highly reassuring for the absence of residual tumor in these areas.

Perhaps the most novel finding of this study is the demonstrated ability of our method to detect subclinical, occult foci of tumor within a lymph node that macroscopically appears normal. The fact that this technique could readily identify tumor deposits of 0.5 x 0.25 mm *ex vivo* could potentially have significant implications in the surgical management of patients with PDAC. Obviously, the sensitivity of this method to detect such occult foci of disease *ex vivo* should be replicated *in vivo* before one can definitively comment on the potential clinical utility of this tool intraoperatively.

As noted above, the main limitation of this study is that all analyzed images to determine the detection threshold for tumor-positive lymph nodes were obtained *ex vivo*. In our previous study, we have shown that it is possible to detect PDAC intra-operatively using clinically available cameras.[5] The smallest tumor size we could detect *in vivo* was a lymph node of 3.0 x 1.2 x 1.0 cm, containing several tumor lesions of different sizes on H&E with the largest focus being 6.8 x 5.6 mm. At this point, the intra-operative fluorescence cameras are not sensitive

enough to detect small amounts of tumor like those used *ex vivo*. The closed-field fluorescent PEARL camera is a highly sensitive camera for imaging of fresh tissue *ex vivo*, and together with the Odyssey NIR fluorescence scanner, these modalities were able to detect minimal amounts of tumor in surgical specimens. There is an obvious need to develop intraoperative cameras that can also reach this degree of sensitivity. Therefore, future development is warranted to improve the performance of intraoperative cameras, and to develop new imaging agents with higher quantum yields resulting in a more intense fluorescent signal. In the future, we hope to reach the aforementioned detection limits with *in vivo* imaging. An additional limitation is the small sample size of this prospective study. However, even though the number of patients was limited, the number of lymph nodes, both positive and negative, was sufficient to show statistically significant and clinically relevant differences.

CONCLUSION

In conclusion, this study provides proof of concept that molecularly targeted fluorescence imaging can detect tumor-positive peripancreatic lymph nodes *ex vivo* with high sensitivity, even in the case of visually occult microscopic disease. Therefore, we believe that this technique, if implemented *in vivo,* has the potential to enhance the surgeon's intraoperative "visibility", thereby enabling better intraoperative staging, and perhaps leading to a more precise and targeted lymph node dissection. Having proven the feasibility and efficacy of intraoperative EGFR-directed molecular fluorescence imaging on patients undergoing resection of pancreatic cancer with this study, and a previous study focusing on detection of the main tumor,[5] our group is in the process of initiating a larger prospective study utilizing EGFR-targeted fluorescent imaging, with the main objective of assessing the frequency by which this intervention can change intraoperative management both in terms of expanding the extent of resection or aborting the resection due to metastatic disease.

FUNDING

We would like to acknowledge support from Stanford Cancer Institute Translational Research Grant, and Intuitive Surgical Clinical Robotics Research Grant. Tummers WS contribution to this work was supported in part by Michaël-van Vloten Fonds, Lisa Waller Hayes Foundation, Jo Kolk Studiefonds, McKinsey Grant, and Ketel1 Studiefonds.

REFERENCES

1. Iacobuzio-Donahue, C.A., et al., DPC4 gene status of the primary carcinoma correlates with patterns of failure in patients with pancreatic cancer. J Clin Oncol, 2009. 27(11): p. 1806-13.
2. Winter, J.M., et al., Survival after resection of pancreatic adenocarcinoma: results from a single institution over three decades. Ann Surg Oncol, 2012. 19(1): p. 169-75.
3. Warram, J.M., et al., Fluorescence imaging to localize head and neck squamous cell carcinoma for enhanced pathological assessment. J Pathol Clin Res, 2016. 2(2): p. 104-12.
4. Rosenthal, E.L., et al., Safety and Tumor-specificity of Cetuximab-IRDye800 for Surgical Navigation in Head and Neck Cancer. Clin Cancer Res, 2015.
5. Tummers, W.S., et al., Intraoperative Pancreatic Cancer Detection Using Tumor-Specific Multimodality Molecular Imaging. Ann Surg Oncol, 2018. in press.
6. Yeo, C.J., et al., Pancreaticoduodenectomy with or without distal gastrectomy and extended retroperitoneal lymphadenectomy for periampullary adenocarcinoma, part 2: randomized controlled trial evaluating survival, morbidity, and mortality. Ann Surg, 2002. 236(3): p. 355-66; discussion 366-8.
7. Yeo, C.J., et al., Pancreaticoduodenectomy with or without extended retroperitoneal lymphadenectomy for periampullary adenocarcinoma: comparison of morbidity and mortality and short-term outcome. Ann Surg, 1999. 229(5): p. 613-22; discussion 622-4.
8. Farnell, M.B., et al., A prospective randomized trial comparing standard pancreatoduodenectomy with pancreatoduodenectomy with extended lymphadenectomy in resectable pancreatic head adenocarcinoma. Surgery, 2005. 138(4): p. 618-28; discussion 628-30.
9. Nimura, Y., et al., Standard versus extended lymphadenectomy in radical pancreatoduodenectomy for ductal adenocarcinoma of the head of the pancreas: long-term results of a Japanese multicenter randomized controlled trial. J Hepatobiliary Pancreat Sci, 2012. 19(3): p. 230-41.
10. Pedrazzoli, S., et al., Standard versus extended lymphadenectomy associated with pancreatoduodenectomy in the surgical treatment of adenocarcinoma of the head of the pancreas: a multicenter, prospective, randomized study. Lymphadenectomy Study Group. Ann Surg, 1998. 228(4): p. 508-17.
11. de Geus, S.W., et al., Selecting Tumor-Specific Molecular Targets in Pancreatic Adenocarcinoma: Paving the Way for Image-Guided Pancreatic Surgery. Mol Imaging Biol, 2016. 18(6): p. 807-819.
12. Tummers, W.S., et al., Selection of optimal molecular targets for tumor-specific imaging in pancreatic ductal adenocarcinoma. Oncotarget, 2017. 8(34): p. 56816-56828.
13. Rosenthal, E.L., et al., Safety and Tumor Specificity of Cetuximab-IRDye800 for Surgical Navigation in Head and Neck Cancer. Clin Cancer Res, 2015. 21(16): p. 3658-66.
14. Moore, L.S., et al., Effects of an Unlabeled Loading Dose on Tumor-Specific Uptake of a Fluorescently Labeled Antibody for Optical Surgical Navigation. Mol Imaging Biol, 2016.
15. Zinn, K.R., et al., IND-directed safety and biodistribution study of intravenously injected cetuximab-IRDye800 in cynomolgus macaques. Mol Imaging Biol, 2015. 17(1): p. 49-57.